DOI 10.1007/s10812-020-00944-0
Journal of Applied Spectroscopy, Vol. 86, No. 6, January, 2020 (Russian Original Vol. 86, No. 6, November–December, 2019)

PHYTOPLANKTON BLOOM AND PHOTOSYNTHETICALLY ACTIVE RADIATION IN COASTAL WATERS

T. Ya. Churilova,[a*] V. V. Suslin,[b] N. A. Moiseeva,[a] and T. V. Efimova[a]

UDC 535.34:581.526.325

The effect of a phytoplankton bloom on the change with depth of photosynthetically available radiation (PAR), the spectral downwelling irradiance in coastal waters, and the phytoplankton ability to absorb PAR in the sea is estimated. The 10-fold increase in the chlorophyll a concentration (from 0.4 to 4.0 mg/m^3) during a diatom/dinoflagellate bloom leads to a decrease in water transparency and a narrowing of the photosynthesis zone. As a consequence, the average PAR within the phytoplankton habitat layer is almost halved. A diatom/dinoflagellate bloom is accompanied by changes in the downwelling irradiance spectrum at the same PAR level (optical depths). The penetrating irradiance maximum near the bottom of the euphotic zone shifts to longer wavelengths (~550–600 nm) as compared to background conditions (~500–550 nm). The increase in diatom/dinoflagellate biomass and the concomitant change in the downwelling irradiance spectrum are accompanied by a decrease in the specific absorption coefficient of phytoplankton pigments up to about three times that under background conditions at the same optical depths. The downwelling irradiance spectrum at fixed optical depths and the ability of cells to absorb light change slightly as compared to background conditions when coccolithophores bloom.

Keywords: *phytoplankton bloom, diatoms, dinoflagellates, coccolithophores, water transparency, solar radiation spectrum, phytoplankton light absorption efficiency, coastal waters.*

Introduction. Coastal waters of all aquifers are susceptible to biogenic elements introduced by surface runoff, which is one of the main factors responsible for the increased phytoplankton content in coastal waters as compared with deep-sea regions of the world [1–3]. An analogous spatial distribution of phytoplankton in the Black Sea was reported [3, 4]. Peaks in phytoplankton populations (biomass) are observed in yearly cycles and are called blooms [5]. Blooms are observed more frequently in coastal waters than on the open seas [3, 6]. Frequent and strong blooms were noted from early spring to late autumn in estuaries of rivers (Danube, Dniepr, Dniestr) on the northwestern Black Sea shelf [7]. The chlorophyll *a* (C_a) concentration during an autumnal bloom of diatoms in coastal waters of Bulgaria and Romania was 3.3–5.4 mg/m^3 [8]. The strongest bloom (C_a ~ 55 mg/m^3) was observed near the mouth of the Dunai River [3], water of which contained significantly more biogenic compounds than other rivers feeding the Black Sea [9]. The C_a content in coastal waters of the Crimean peninsula (Black-Sea sector) was typically much lower and varied from 0.25 to 3.5 mg/m^3 during a year [10]. The C_a = 2–4 mg/m^3 in Sevastopol Bay waters during spring and autumnal blooms of diatoms [11]. Higher C_a values of 5–8 mg/m^3 were noted only at separate stations located in areas affected by Chernaya River or domestic runoffs [12, 13].

A bloom in the Black Sea was associated with the development of species in the classes *Bacillariophyceae, Dinophyceae*, and *Coccolithophyceae* (*Primnesiophyceae*) [3, 7, 11, 12]. Coccolithophores are notable for their optical properties and are capable of scattering an order of magnitude more light than other taxonomic species [14]. The optical properties of phytoplankton cells (ability to absorb and scatter light) affect the quantitative characteristics of a light field in aquifers [15]. Measurements of Secchi disk visibility and/or beam attenuation coefficient at a particular wavelength that were taken in the Black Sea [16, 17] and other global oceans [18, 19] showed that water transparency depends on the phytoplankton biomass. The relationship between the C_a concentration, which was used as an indicator of phytoplankton biomass, and the

*To whom correspondence should be addressed.

[a]A. O. Kovalevsky Institute of Biology of the Southern Seas, Russian Academy of Sciences, Sevastopol, 299011, Crimea, Russia; email: tanya.churilova@gmail.com; [b]Marine Hydrophysical Institute, Russian Academy of Sciences, Sevastopol, 299011, Crimea, Russia. Translated from Zhurnal Prikladnoi Spektroskopii, Vol. 86, No. 6, pp. 976–985, November–December, 2019. Original article submitted April 10, 2019.

water transparency index was not constant [16, 17]. It varied because of the ratio between phytoplankton and other optically active constituents, i.e., colored dissolved organic matter (CDOM) and suspended nonliving particulate matter (NAP) [18, 19], and because the specific (calculated for C_a) ability of phytoplankton to absorb light changed [20]. Studies of the diffuse attenuation coefficients [$K_d(\lambda)$] and downwelling irradiance [$E_d(\lambda)$] showed that increased phytoplankton biomass not only reduced the transparency but also changed the spectrum of downwelling irradiance. The maximum in the $E_d(\lambda)$ spectrum at a depth with 1% photosynthetically active radiation (PAR) shifted from ~490 nm in depleted water to longer wavelengths (~550 nm) in more productive waters [20]. The illumination conditions were shown to affect the specific absorption efficiency by phytoplankton pigments (a^*_{ph}) in the sea [20]. The spectral properties of the light field and the absorption efficiency of phytoplankton pigments have substantial effects on primary production of the waters [21]. However, only anecdotal studies of the variability of a^*_{ph} in natural aquifers are known [20] and are altogether missing for the Black Sea. The spectral coefficients of light attenuation [$K_d(\lambda)$] and downwelling irradiance [$E_d(\lambda)$] in the Black Sea were measured only recently [22, 23] because the spectroradiometers were designed [23] or acquired [22] comparatively recently. It is noteworthy that simultaneous measurements of the light spectrum and absorption coefficients of phytoplankton pigments in the Black Sea are still unknown although they are needed to estimate correctly the amount of PAR quanta absorbed by phytoplankton. However, many measurements of spectral coefficients $a_{ph}(\lambda)$, $a_{NAP}(\lambda)$, and $a_{CDOM}(\lambda)$ taken in the Black Sea [10, 24, 25] provided basic information for simulating the diffuse attenuation [$K_d(\lambda)$] and downwelling irradiance coefficients [$E_d(\lambda)$] using an algorithm that reproduced highly accurately the $E_d(\lambda)$ spectra [26].

New data on the effect of phytoplankton blooms on the spectrum of solar radiation penetrating into the sea could be obtained by using the measured biooptic coefficients $a_{ph}(\lambda)$, $a_{NAP}(\lambda)$, and $a_{CDOM}(\lambda)$ of Crimean coastal waters and simulated coefficients $K_d(\lambda)$ and $E_d(\lambda)$. The effects of the light-field spectral characteristics on the specific absorption efficiency of phytoplankton pigments, which determined the photosynthesis rate and phytoplankton primary production, could be estimated [27].

The goal of the present work was to study the effects of a phytoplankton bloom on the PAR in the sea and its spectrum and on the specific (calculated for the C_a concentration and total amount of available PAR quanta) absorption efficiency of light by phytoplankton pigments in coastal waters of the Black Sea in the Crimean region.

Experimental. Biooptic data obtained in coastal waters of the Black Sea in the Crimean region during expeditions on the SRV Professor Vodyanitsky on Apr. 19–25, Jun. 8–18, and Oct. 26–30, 2016, were used. The chlorophyll *a* concentration together with pheopigments (C_a) was determined by spectrophotometry [28]. Coefficients $a_{ph}(\lambda)$ by NAP [$a_{NAP}(\lambda)$ and $a_{CDOM}(\lambda)$] were determined using a NASA protocol [29]. Measurements were made on a Lambda 35 dual-beam spectrophotometer (PerkinElmer) with an integrating sphere. Spectra of $a_{NAP}(\lambda)$ and $a_{CDOM}(\lambda)$ displayed exponential dependences. Coefficients of the exponent (S_{NAP} and S_{CDOM}) were calculated for the ranges 400–700 and 350–500 nm. The hydrophysical and biooptic parameters were mainly homogeneously distributed in coastal water at depths up to ~50 m because of the active hydrodynamics of coastal waters [30].

Two scenarios were simulated to estimate the effect of phytoplankton biomass on water transparency, downwelling irradiance intensity and spectrum, and specific efficiency of light absorption by phytoplankton.

1. Bloom of microalgae of classes *Bacillariophyceae* and *Dinophyceae*. The quantity C_a, which varied from 0.4 to 4.0 mg/m^3 according to the noted variability of this parameter in Crimean coastal waters during the warm months of 2016, was used as an indicator of phytoplankton biomass that detected a bloom [10]. The background conditions where C_a = 0.4 mg/m^3 were considered a control (Fig. 1). Increases of C_a from 2 to 10 times ($k2$–$k10$) that of the control were analyzed.

2. Bloom of coccolithophores (class *Coccolithophyceae*). In this instance, an increase of the fraction (N_{cocco}) of this taxon in the total cell population in the phytoplankton community from 0.1 to 1 was used and corresponded to a coccolithophore bloom when the coccolithophore cell concentration increases whereas the contents of other phytoplankton species drops to zero. The quantity C_a in this scenario did not change. This is often observed during a coccolithophore bloom at the start of summer [31]. The shape of $a_{ph}(\lambda)$ did not change if the phytoplankton species profile changed. This assumption was acceptable because species in classes *Bacillariophyceae, Dinophyceae*, and *Coccolithophyceae* have pigment compositions that differ in auxiliary pigments. The specific pigment (pigment marker) of diatom algae (*Bacillariophyceae*) is fucoxanthin; of dinoflagellates (*Dinophyceae*), peridinin; of coccolithophores (*Coccolithophyceae*), 19-hexanoloxyfucoxanthin [32]. However, absorption bands in spectra of these pigments have practically the same positions, which explains the lack of significant differences in the shape of $a_{ph}(\lambda)$ upon changing the species under identical solution conditions [33].

The vertical attenuation spectral diffusion coefficient $K_d(\lambda)$ was calculated as before [34]:

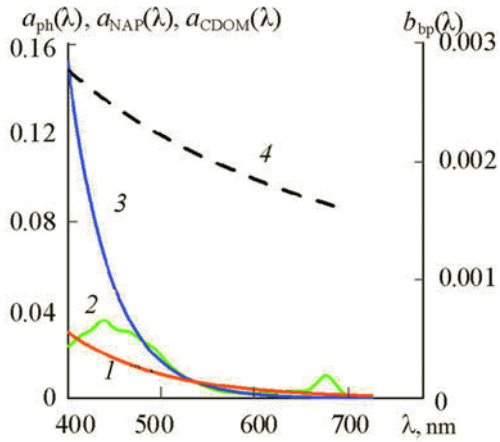

Fig. 1. Background biooptic conditions (control) in Black Sea coastal waters: visible absorption spectrum of suspended particulate matter $a_{NAP}(\lambda)$ (1), phytoplankton pigments $a_{ph}(\lambda)$ (2), and colored dissolved organic matter $a_{CDOM}(\lambda)$ (3) and light back-scattering index of suspended particulates $b_{bp}(\lambda)$ (4).

$$K_d(\lambda) = 1.2(a(\lambda) + b_b(\lambda)), \quad (1)$$

where $b_b(\lambda)$ is the light-scattering coefficient in the rear hemisphere that includes scattering by H_2O [$b_{bw}(\lambda)$] [35] and particulates [$b_{bp}(\lambda)$]; $a(\lambda)$, marine water absorption coefficient that consists of the sum of suspended matter absorption coefficient $a_p(\lambda)$, dissolved organic matter $a_{CDOM}(\lambda)$, and pure water $a_w(\lambda)$ [36] in the visible range 400–700 nm and is determined by the formula [15]:

$$a(\lambda) = a_w(\lambda) + a_p(\lambda) + a_{CDOM}(\lambda),$$

$a_p(\lambda) = a_{ph}(\lambda) + a_{NAP}(\lambda)$. The $a_{ph}(\lambda)$ spectrum was reproduced using highly resolved (1 nm) C_a values and the exponential function relating these parameters [37]:

$$a_{ph}(\lambda) = A(\lambda)\, C_a^{B(\lambda)},$$

where $A(\lambda)$ and $B(\lambda)$ are parametric coefficients of the relationship between C_a and $a_{ph}(\lambda)$ in the warm period (Table 3 [24]), which was acceptable for coastal water phytoplankton [10].

Spectra $a_{NAP}(\lambda)$ and $a_{CDOM}(\lambda)$ calculated as average spectra for data obtained in the warm period of 2016 were used in the calculations (Fig. 1). Spectra $a_{NAP}(\lambda)$ and $a_{CDOM}(\lambda)$ obeyed the exponential function $a_i(\lambda) = a_i(440) \exp[-S_i(\lambda - 440)]$, i is NAP or CDOM with exponent coefficients $S_{NAP} = 0.010$ nm^{-1} and $S_{CDOM} = 0.022$ nm^{-1} and absorption coefficients for $\lambda = 440$ nm $a_{NAP}(440) = 0.020$ m^{-1} and $a_{CDOM}(440) = 0.063$ m^{-1}.

The quantity $b_{bp}(\lambda)$ was calculated according to the literature [14]:

$$b_{bp}(\lambda) = b_{bp}(\lambda_0)\lambda_0/\lambda,$$

where $\lambda_0 = 555$ nm; $b_{bp}(555) = 0.030$ m^{-1} for the coccolithophore phytoplankton community or 0.002 m^{-1} for diatom/dinoflagellate [14]. The quantity $b_{bp}(555)$ for a coccolithophore bloom was calculated using the increase of N_{cocco} from 0.1 to 1:

$$b_{bp}(555) = 0.002(1 - N_{cocco}) + 0.030N_{cocco}.$$

The quantity $K_d(\lambda)$ calculated using Eq. (1) was used to determine illuminance spectra at depths (z) $E_d(\lambda, z)$ in the layer at 0–50 m in 1-m steps according to the exponential nature of the change of illuminance with depth [15]:

$$E_d(\lambda, z) = E_d(\lambda, 0^-) \exp(-K_d(\lambda)z), \quad (2)$$

where $E_d(\lambda, 0^-)$ is spectrum $E_d(\lambda, z)$ immediately below the sea surface. Spectrum $E_d(\lambda, 0^-)$ was reproduced based on the daily PAR = 57.8 E/(m^2·d) [38] and spectral characteristics of $E_d(\lambda, 0^-)$ typical for Crimean latitudes [39] considering the conversion from energy units to number of quanta. The change of PAR with depth was calculated for the layer at 0–50 m in 1-m steps using the formula [15]:

$$\mathrm{PAR}(z) = \int_{400}^{700} E_d(\lambda, z)d\lambda \ .$$

The average PAR for the upper quasi-homogeneous layer (in our instance, for the layer from the surface to the bottom, 0–50 m) is found using the equation [40]:

$$\mathrm{PAR_{ML}} = \mathrm{PAR}(0^-)\frac{\left(1 - \exp\left\{-4.6z_{ml}/z_{eu}\right\}\right)}{4.6z_{ml}/z_{eu}} \ .$$

The optical depth was defined as the product of z and K_d [15] calculated using Eq. (2) but for the PAR. The lower limit of the zone (z_{eu}) was taken as the depth where the illuminance was 1% of the PAR level incident on the sea surface; the optical depth, 4.6.

The specific absorption efficiency by phytoplankton pigments ($\overline{a}^*_{\mathrm{ph}}$, $\mathrm{m^2/mg}$), which characterized the number of absorbed quanta per unit concentration C_a and unit PAR quanta flux density, was calculated using the formula [41]:

$$\overline{a}^*_{\mathrm{ph}}(z) = \frac{\int_{400}^{700} a_{ph}(\lambda, z)E_d(\lambda, z)d\lambda}{C_a\int_{400}^{700} E_d(\lambda, z)d\lambda} \ .$$

Results and Discussion. The C_a values in Crimean coastal waters varied by more than an order of magnitude and reached 3.5–4.0 $\mathrm{mg/m^3}$ during a bloom. The phytoplankton-pigment absorption coefficients for C_a = 0.4 $\mathrm{mg/m^3}$ at the blue (λ ~ 440 nm) and red maxima (λ ~ 678 nm) were 0.034 and 0.096 $\mathrm{m^{-1}}$ (Fig. 1). Light absorption by NAP and CDOM at ~440 nm, which corresponded to the maximum absorption by phytoplankton pigments, were a_{NAP} = 0.020 $\mathrm{m^{-1}}$ and a_{CDOM} = 0.063 $\mathrm{m^{-1}}$ (Fig. 1). Spectra $a_{\mathrm{NAP}}(\lambda)$ and $a_{\mathrm{CDOM}}(\lambda)$ were exponential in shape. The exponent coefficients (S) were determined to parametrize these spectra and were 0.010 $\mathrm{nm^{-1}}$ for $a_{\mathrm{NAP}}(\lambda)$ and 0.022 $\mathrm{nm^{-1}}$ for $a_{\mathrm{CDOM}}(\lambda)$.

Coefficients $a_{\mathrm{ph}}(\lambda)$ and $b_{\mathrm{bp}}(\lambda)$ increased during a diatom/dinoflagellate bloom, which increased $K_d(\lambda)$ (Fig. 2) and altered the shape of the spectrum. This was most significant in the short-wavelength visible region (~440 nm) (Fig. 2), which corresponded to the absorption maximum of phytoplankton pigments (Fig. 1). Layer z_{eu} compressed from 40 m in the control to 35 m upon doubling C_a ($k2$) as a result of increasing $K_d(\lambda)$. The euphotic zone for C_a = 4.0 $\mathrm{mg/m^3}$ ($k10$) was 20.5 m, i.e., about twice as narrow as the control.

Parameter $b_{\mathrm{bp}}(\lambda)$ was affected by a change of coccolithophore fraction in the phytoplankton community during a coccolithophore bloom. In this scenario, C_a and $a_{\mathrm{ph}}(\lambda)$ did not change. Figure 2 shows the change of $K_d(\lambda)$ and $E_d(\lambda)$ during a coccolithophore bloom. The euphotic zone z_{eu} = 38 m and differed insignificantly from the control (40 m) with a coccolithophore fraction of 0.1 (k = 0.1) in the total phytoplankton population. If the whole phytoplankton community was coccolithophores (k = 1), then z_{eu} = 30 m.

Increasing $K_d(\lambda)$ and narrowing the euphotic layer altered the lighting conditions in the habitat layer of phytoplankton that were mixed from the sea surface to the bottom in the hydrodynamically active coastal water because they were a passive suspension. In this instance, the lighting conditions in the phytoplankton habitat were average illuminance for a mixed layer ($\mathrm{PAR_{ML}}$). The quantity $\mathrm{PAR_{ML}}$ was halved [from 10 to 5.2 $\mathrm{E/(m^2 \cdot d)}$] during a diatom/dinoflagellate bloom (Fig. 3). A coccolithophore bloom was accompanied by less pronounced (by ~20%) attenuation of $\mathrm{PAR_{ML}}$ from 10 to 7.4 $\mathrm{E/(m^2 \cdot d)}$ (Fig. 3).

The change of $K_d(\lambda)$ and the shape of its spectrum caused not only a narrowing of the illuminated layer but also a change of the irradiance spectrum in the sea (Fig. 2). The shapes of $E_d(\lambda)$ were compared at depths with identical PAR levels, i.e., at the same optical depths, to find differences in the shape of $E_d(\lambda)$ related to a phytoplankton bloom. Radiation in the range 500–540 nm primarily penetrated in the control at a depth with 1% illuminance (Fig. 2). The increase of C_a from 0.4 to 4.0 $\mathrm{mg/m^3}$ during a diatom/dinoflagellate bloom changed the shape of the $E_d(\lambda)$ spectrum (Fig. 2) whereas a coccolithophore bloom had practically no effect on $E_d(\lambda)$. The downwelling-irradiance maximum shifted to longer wavelengths during a diatom/dinoflagellate bloom. The downwelling-irradiance maximum shifted by ~10 nm if C_a was doubled ($k2$); by ~50 nm, for an order of magnitude ($k10$) (Fig. 2).

The irradiance spectrum in the sea has a considerable influence on the ability of phytoplankton to absorb solar energy (Fig. 4). The quantity $\overline{a}^*_{\mathrm{ph}}$ in the control changed from 0.031 $\mathrm{m^2/kg}$ in the surface layer to 0.038 $\mathrm{m^2/mg}$ at optical depth 4.6. It decreased markedly with increasing C_a during a diatom/dinoflagellate bloom (Fig. 4). The quantity $\overline{a}^*_{\mathrm{ph}}$ in the surface layer

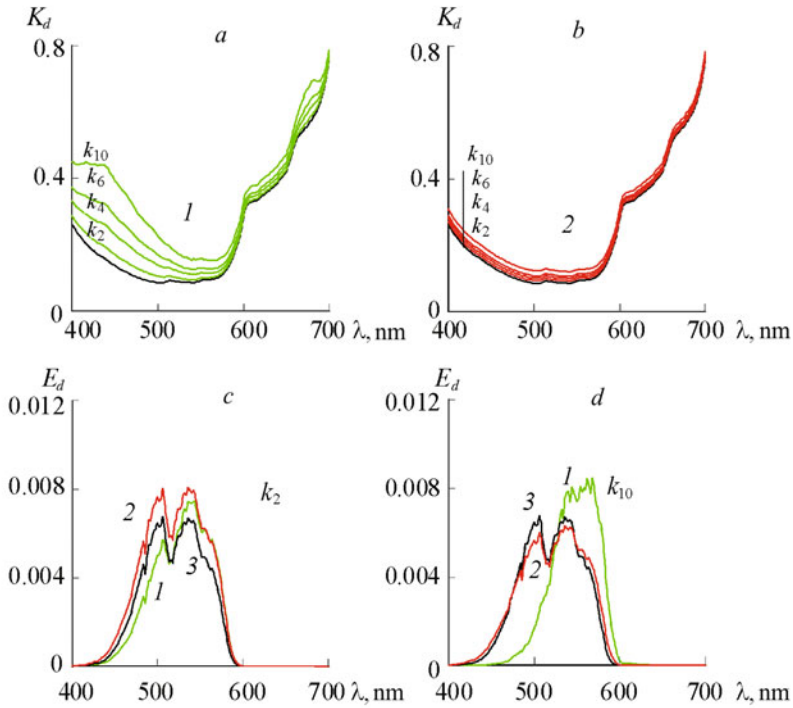

Fig. 2. Spectra of vertical attenuation index of solar radiation in the sea $K_d(\lambda)$ (a, b) and quantum illuminance $E_d(\lambda)$ [E/(m^2·d·nm)] at optical depth 4.6 (c, d); k is the multiple increase of chlorophyll a concentration during a diatom/dinoflagellate bloom (1) or fractions of coccolithophores in the total population of phytoplankton cells during a coccolithophore bloom (2) as compared to the control (3).

decreased from 0.031 in the control to 0.028 m^2/mg if C_a was doubled ($k2$). Increasing C_a by an order of magnitude ($k10$) decreased $\overline{a}^*_{ph}$ in the surface layer to 0.022 m^2/mg, which was ~30% less than in the control. The most pronounced (by almost three times) decrease of $\overline{a}^*_{ph}$ occurred for the lower limit of the euphotic zone, i.e., at optical depth 4.6. The quantity $\overline{a}^*_{ph}$ decreased from 0.033 in the control to 0.025 m^2/mg for $k2$ and 0.012 m^2/mg for $k10$. A coccolithophore bloom had practically no effect on $\overline{a}^*_{ph}$ (Fig. 4) and its change with optical depth, in contrast with a diatom/dinoflagellate bloom. This was related to the lack of noticeable changes of $E_d(\lambda)$ at constant optical depths (Fig. 2).

A comparison of the effects of a phytoplankton bloom on the light spectrum in coastal waters revealed common changes and several features associated with the taxonomic classification of the blooming species. The common changes included reduced water transparency and; therefore, a decreased illuminated zone in the mixed layer from the sea surface to the bottom. This decreased the illuminance in the phytoplankton habitat.

Phytoplankton can undergo cellular transformations to adapt to changes in the lighting conditions of their habitat [42]. An estimate based on the dependences of the ratio between C_a and organic carbon (Chl/C) in phytoplankton cells on illuminance [43] showed that the Chl/C ratio in algal cells increased ~1.7 times if the illuminance was approximately halved (Fig. 3), which was noted for a 10-fold increase of C_a during a diatom/dinoflagellate bloom ($k10$). This meant that the phytoplankton biomass increased less than C_a during a diatom/dinoflagellate bloom. The illuminance in the habitat layer changed less significantly for a coccolithophore bloom (Fig. 3). Therefore, the adaptive response of the algal cells was less pronounced than for a diatom/dinoflagellate bloom. These differences arose because the increase of C_a from 0.4 to 4.0 mg/m^3 during a diatom/dinoflagellate bloom was accompanied by increased absorption by phytoplankton $a_{ph}(\lambda)$ almost to the same degree as C_a (almost an order of magnitude). Coefficient $b_{bp}(\lambda)$ for a coccolithophore bloom increased as the fraction (N) of this species in the total phytoplankton population increased (by an order of magnitude for k = 10). The background coefficients $a_{ph}(\lambda)$ and $b_{bp}(\lambda)$ differed by almost an order of magnitude (Fig. 1). Also, the differences in the effect of the bloom of these taxa on water transparency and lighting conditions in the phytoplankton habitat determined the shapes of their spectra.

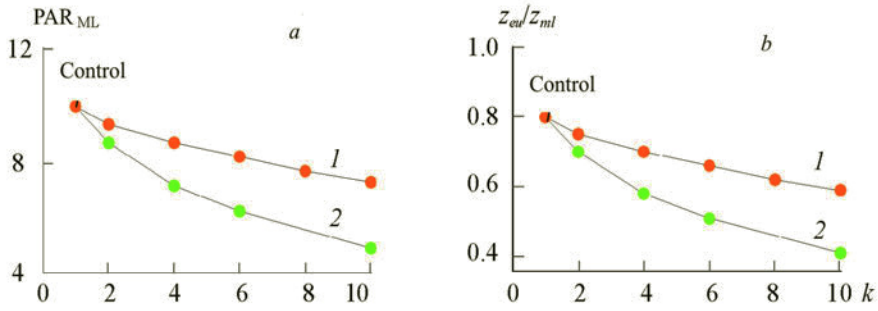

Fig. 3. Effects of relative population (k) of coccolithophores (1) or chlorophyll a concentration during a diatom/dinoflagellate bloom (2) on the average PAR in the mixed layer (PAR_{ML}, E/(m^2·d)) (a) and narrowing of the illuminated layer (z_{eu}/z_{ml}) (b).

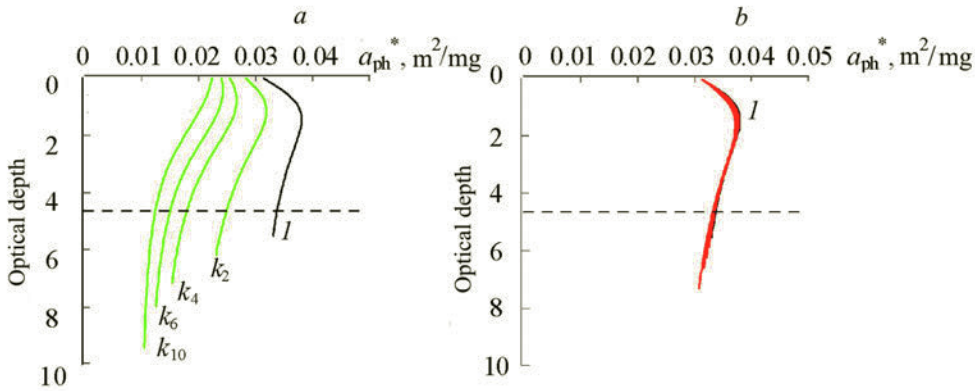

Fig. 4. Change of specific (normalized to chlorophyll a and PAR concentrations) efficiency of light absorption by phytoplankton pigments a_{ph}^* as a function of optical depth during diatom/dinoflagellate (a) and coccolithophore blooms (b) as compared to the control (1) with different multiple increases (k) of coccolithophore cell fraction or chlorophyll a concentration during a bloom; dashed lines show optical depth 4.6.

Coccolithophores and diatom/dinoflagellates showed considerable differences in their influence on the spectrum of downwelling solar radiation with depth (Fig. 2). The results indicated that the light spectral characteristics were a critical factor determining the photosynthetic potential of algae. The same number of PAR quanta with different spectra are absorbed with different specific efficiencies by phytoplankton pigments (Fig. 4). A diatom/dinoflagellate bloom shifts the downwelling radiation maximum to longer wavelengths. Cell pigments at C_a = 4 mg/m^3 (k10) absorb radiation in the range 550–600 nm penetrating to optical depth 4.6 with efficiency about three times less than the control (at C_a = 0.4 mg/m^3) or during a coccolithophore bloom, when radiation in the range 500–550 nm penetrates to this same optical depth (Fig. 2). It is noteworthy that a_{ph}^* in the sea surface layer decreases by ~30% if C_a increases by an order of magnitude. The observed decrease of a_{ph}^* is related to the effect of the pigment concentration on the light absorption efficiency by phytoplankton cells because light in the sea surface layer is practically white [37]. The quantity a_{ph}^* decreases by about three times near the lower limit of the euphotic layer. Therefore, the change of downwelling radiation spectrum caused by the increased phytoplankton biomass turns out to be a more critical factor that interferes with the ability of phytoplankton to utilize light quanta for photosynthesis.

Until now, the photosynthetic and production characteristics of phytoplankton in the Black Sea were studied relative to the total amount of PAR in the sea without considering its spectrum [44]. Primary production (PP) was estimated using a radiocarbon method with exposure *in situ* [44] or simulated conditions in a laboratory experiment with brief exposure in a special incubator that allowed the phytoplankton photosynthetic characteristics, i.e., photosynthesis efficiency, maximum photosynthesis rate, and light intensity saturating photosynthesis [8], to be determined at various depths. The change of PP with depth in the sea was calculated based on the dependence of these photosynthetic characteristics on PAR [8]. However,

the variability of the photosynthetic characteristics was studied without considering the change of light spectrum [8]. This reduced the accuracy of the PP estimate with non-white light. The PAR decreases with depth on a greater gradient than in transparent waters if the contents of phytoplankton (C_a) and other optically active medium constituents (NAP and CDOM) increase [45, 46]. The productive layer narrows to several meters because of rapid attenuation of light in turbid waters [45, 46]. Moreover, rapid attenuation of light in turbid waters is accompanied by a change in the spectrum starting from the surface layer according to the present studies (Fig. 2) and previous work [47]. Obviously, an estimate of the lighting conditions for phytoplankton and the photosynthesis rate, which is determined by the number of absorbed quanta and the quantum yield [21, 27], should consider the light spectrum and the light-absorbing capability of the phytoplankton.

Conclusions. The light spectrum was shown to change during a bloom of species in the classes *Bacillariophyceae, Dinophyceae*, and *Coccolithophyceae*. The specific light-absorption efficiency by phytoplankton was estimated for the first time and shown to vary because of a change in the light spectrum in the sea. The results could be used to predict ecological consequences due to the influence of anthropogenic factors on the intensity and frequency of phytoplankton blooms. Additional indicators that in combination with C_a and the water transparency coefficient provide a more informative estimate of the habitat quality of planktonic and benthic algae must be elaborated to evaluate the ecological situation of coastal waters.

Acknowledgments. The work was performed on a State Task Topic (State Reg. No. AAAA-A18-118020890112-1), Study of Space-Time Organization of Aquatic and Terrestrial Ecosystems to Develop Real-time Monitoring Systems Based on Remote Sensing Data and GPS Technologies, Reg. No. AAAA-A19-119061190081-9 and topic Development of Regional Algorithms for Replicating Biooptic Characteristics of the Black Sea (in combination with Development of Methods and Means of Real-time Oceanology to Study Black Sea Field Variability), Reg. No. AAAA-A18-118020890112-1, and was sponsored in part by the Russian Foundation for Basic Research (Grants No. 17-05-00113, 18-45-920070, and 18-05-80025).

REFERENCES

1. T. R. Parsons, M. Takahashi, and B. Hargrave, *Biological Oceanographic Processes*, Pergamon Press, Oxford (1977).
2. J. E. G. Raymont, *Plankton and Productivity in the Oceans*, 2nd edn., Pergamon, Oxford (1980).
3. S. Moncheva, O. Gotsis-Skretas, K. Pagou, and A. Krastev, *Estuarine Coastal Shelf Sci.*, **53**, 281–295 (2001).
4. L. V. Georgieva, *Black Sea Plankton* [in Russian], Naukova Dumka, Kiev (1993), pp. 31–55.
5. T. J. Smayda, *Limnol. Oceanogr.*, **42**, No. 5, Pt. 2, 1132–1136 (1997).
6. J. G. Ferreira, J. H. Andersen, A. Borja, S. B. Bricker, J. Camp, M. Cardoso da Silva, and U. Claussen, *Estuarine Coastal Shelf Sci.*, **93**, No. 2, 117–131 (2011); doi: 10.1016/j.ecss.2011.03.014.
7. Yu. P. Zaitsev, B. G. Aleksandrov, and G. G. Minicheva (Eds.), *Phytoplankton: Open Regions. Northwestern Black Sea: Biology and Ecology* [in Russian], Naukova Dumka, Kiev (2006), pp. 175–184.
8. Z. Z. Finenko, T. Ya. Churilova, A. V. Parkhomenko, and S. Tugrul, *Morsk. Ekol. Zh.*, No. 4, 75–84 (2008) [in English].
9. BSC, 2008. *State of the Environment of the Black Sea (2001-2 2006/7)*, Temel Oguz (Ed.), Publications of the Commission on the Protection of the Black Sea Against Pollution (BSC) 2008-3 3, Istanbul, Turkey (2008), p. 448.
10. T. Churilova, N. Moiseeva, T. Efimova, V. Suslin, O. Krivenko, and E. Zemlianskaia, *23rd Int. Symp. Atmospheric and Ocean Optics, Atmospheric Physics*, 104664B, Nov. 30, 2017, (2017); doi 10.1117/12.2288339, URL: http://dx.doi.org/10.1117/12.2288339.
11. Z. Z. Finenko, L. V. Stelmakh, I. M. Mansurova, E. Yu. Georgieva, and V. S. Tsilinskii, *Sist. Kontrolya Okruzh. Sredy*, No. 9 (29), 73–82 (2017).
12. L. V. Stel′makh, I. I. Babich, and S. V. Lyashenko, *Ekol. Morya*, **61**, 64–68 (2002).
13. A. A. Dzhulai, *Ecological Safety of Coastal and Shelf Zones and Comprehensive Use of Shelf Resources*, No. 25–2 (2011), pp. 357–369.
14. V. I. Man′kovskii, *Principles of Ocean Optics* [in Russian], Marine Hydrophysical Inst., Izd. Sevastopol (1996), p. 119.
15. J. T. O. Kirk, *Light and Photosynthesis in Aquatic Ecosystem*, UK Cambridge University Press, Cambridge (2011), Vol. 3.
16. V. I. Man′kovskii, E. V. Man′kovskaya, and M. V. Solov′ev, *Hydrooptic Characteristics of the Black Sea, Handbook* [in Russian], MGI NAN Ukrainy, Sevastopol (2009).
17. A. S. Kukushkin, *Opt. Atmos. Okeana*, **26**, No. 2, 113–123 (2013).
18. W. Wang and J. Zhao, *Acta Oceanol. Sin.*, **33**, No. 6, 53–62 (2014); doi: 10.1007/s13131-014-0489-3.
19. E. T. Harvey, J. Walve, A. Andersson, B. Karlson, and S. Kratzer, *Front. Mar. Sci.*, **5**, 496 (2019); doi: 10.3389/fmars.2018.00496.

20. A. U. Bracher and M. M. Tilzer, *Polar Biol.*, **24**, No. 9, 687–696 (2001).
21. A. Morel, *Prog. Oceanogr.*, **26**, 263–306 (1991).
22. S. V. Vazyulya and S. V. Sheberstov, in: *Proceedings of the IXth All-Russian Conf. "Current Problems of Natural Water Optics"* [in Russian], September 20–22, 2017, St. Petersburg (2017), pp. 229–234.
23. V. V. Suslin, A. A. Latushkin, and O. V. Martynov, in: *24th Int. Symp. Atmospheric and Ocean Optics: Atmospheric Physics*, 108333I, Dec. 13, 2018 (2018); doi: 10.1117/12.2503272; https://doi.org/10.1117/12.2503272.
24. T. Churilova, V. Suslin, O. Krivenko, T. Efimova, N. Moiseeva, V. Mukhanov, and L. Smirnova, *Front. Mar. Sci.*, **4**, 90 (2017); doi: 10.3389/fmars.2017.00090.
25. T. Churilova, V. Suslin, H. M. Sosik, T. Efimova, N. Moiseeva, S. Moncheva, V. Mukhanov, O. Rylkova, and O. Krivenko, *Eur. J. Remote Sens.*, **52**, Suppl. 1, 123–136 (2019); doi: 10.1080/22797254.2018.1533389.
26. T. Churilova, V. Suslin, and H. M. Sosik, *Phys. Oceanogr.*, **19**, No. 6, 366–378 (2009).
27. T. Ya. Churilova, V. V. Suslin, O. V. Krivenko, T. V. Efimova, and N. A. Moiseeva, *Zh. Sib. Fed. Univ., Biol.*, **9**, No. 4, 367–384 (2016).
28. S. W. Jeffrey and G. F. Humphrey, *Biochem. Physiol. Pflanz.*, **167**, 191–197 (1975); doi: 10.1016/S0015-3796(17)30778-3.
29. B. G. Mitchell, M. Kahru, J. Wieland, and M. Stramska, NASA Goddard Space Flight Center (2003), pp. 39–64.
30. V. A. Ivanov and V. N. Belokopytov, *Oceanography of the Black Sea*, National Academy of Sciences of Ukraine, Marine Hydrophysical Institute, Sevastopol (2011), p. 210.
31. G. P. Berseneva, T. Ya. Churilova, and L. V. Georgieva, *Okeanologiya*, **44**, No. 3, 389–398 (2004).
32. S. W. Jeffrey, R. F. C. Mantoura, and S. W. Wright (eds.), *Phytoplankton Pigments in Oceanography: Guidelines to Modern Methods*, UNESCO Publishing (1997), p. 661.
33. T. Ya. Churilova, Z. Z. Finenko, and A. I. Akimov, EKOSI-Gidrofizika, (2008), pp. 301–319.
34. H. R. Gordon, O. B. Brown, R. H. Evans, J. W. Brown, R. S. Smith, K. S. Baker, and D. K. Clark, *J. Geophys. Res.*, **93**, No. D9, 10909–10924 (1988).
35. R. C. Smith and K. S. Baker, *Appl. Opt.*, **20**, 177–184 (1981).
36. R. M. Pope and E. S. Fry, *Appl. Opt.*, **36**, 8710–8723 (1997).
37. A. Bricaud, M. Babin, A. Morel, and H. Claustre, *J. Geophys. Res.*, **100**, C7, 13321–13332 (1995).
38. V. V. Suslin, S. N. Korolev, A. A. Kucheryaviy, T. Ya. Churilova, and O. V. Krivenko, in: *21st Int. Symp. Atmospheric and Ocean Optics: Atmospheric Physics*, Nov. 19, 2015 (2015); http://dx.doi.org/10.1117/12.2203660.
39. K. S. Shifrin, *Optics of the Ocean, Physics of the Ocean* [in Russian], Nauka, Moscow (1978), Vol. 1, pp. 340–396.
40. M. Babin, A. Morel, H. Claustre, A. Bricaud, Z. Kolber, and P. Falkowski, *Deep-Sea Res.*, **43**, 1241–1272 (1996).
41. D. Atlas and T. T. Bannister, *Limnol. Oceanogr.*, **25**, 157–159 (1980).
42. H. L. MacIntyre, T. M. Kana, J. Anning, and R. Geider, *J. Phycol.*, **38**, 17–38 (2002).
43. M. J. Behrenfeld, R. T. O'Malley, E. S. Boss, T. K. Westberry, J. R. Graff, K. H. Halsey, A. J. Milligan, D. A. Siegel, and M. B. Brown, *Nat. Clim. Change*, **6**, No. 3, 323–330 (2015); doi:10.1038/nclimate2838.
44. Yu. I. Sorokin, *The Black Sea: Ecology and Oceanography. Biology of Inland Waters*, Backhuys Publishers, Leiden (The Netherlands) (2002), p. 875; ISBN: 90–5782–105–2.
45. V. D. Chmyr, A. S. Bologa, Z. P. Burlakova, and V. I. Kholodov, *Primary Production of the Western Part of the Sea in Spring. Water Dynamics and Phytoplankton Productivity of the Black Sea* [in Russian], IOAN SSSR, Moscow (1988), pp. 301–314.
46. C. Gameiro, J. Zwolinski, and V. Brotas, *Hydrobiologia*, **669**, 249–263 (2011); doi: 10.1007/s10750-011-0695-3.
47. T. Churilova, V. Suslin, N. Moiseeva, and T. Efimova, in: *24th Int. Symp. Atmospheric and Ocean Optics: Atmospheric Physics*, 1083365, December 13, 2018 (2018); doi: 10.1117/12.2504637.